Environ Earth Sci (2016) 75:1126
DOI 10.1007/s12665-016-5930-9

THEMATIC ISSUE

Scenario-based runoff prediction for the Kaidu River basin of the Tianshan Mountains, Northwest China

Changchun Xu[1] · Jie Zhao[1] · Haijun Deng[2] · Gonghuan Fang[2] · Jing Tan[3] · Dandan He[1] · Yapeng Chen[2] · Yaning Chen[2] · Aihong Fu[2]

Received: 19 November 2015 / Accepted: 23 July 2016

Abstract Based on the hydro-meteorological data over the past 50 years (1961–2010), the runoff change of the Kaidu River was predicted for the future 30 years (2011–2040). Two statistical downscaling models, the Statistical DownScaling Model (SDSM) and the Statistical Analog Resampling Scheme (STARS), were used to downscale the HadCM3 outputs for projecting the future climate scenarios of the basin. The Soil and Water Assessment Tool (SWAT) hydrological model was driven by the projected climate scenarios to generate the future runoff. Modeling results suggested that the SWAT model can well duplicate the recorded runoff changes in the basin and thus can be applied to simulation of future runoff changes. Both the SDSM and the STARS models performed well in simulating the temperature but relatively poorly in simulating the precipitation. Under the A2 and B2 scenarios the basin will experience a significant increasing trend in temperature and an indistinctive change trend in precipitation during the entire forecast period. Under the S1–S3 scenarios, both temperature and precipitation do not exhibit distinctive changes. In terms of river runoff, the predicted average annual runoff will be relatively abundant during the period from 2010s to 2020s but obviously short after 2020s under A2 scenario and will be kept relatively steady under B2 scenario. The predicted runoff will fluctuate drastically with no any significant trend under S1–S3 scenarios. The relatively high runoffs under S2–S3 scenarios seem to indicate the importance of temperature increasing in generating runoff. The scenario-based predictions suggest that moderate emission (e.g., B2) or moderate warming (e.g., S2) is beneficial to maintaining the expected level of runoff in the future.

Keywords SWAT · Statistical downscaling · Runoff prediction · Kaidu River

Introduction

The current water-related problems facing humanity, such as flood disasters, water shortage and water-related ecological deterioration, are mostly resulted from the human disturbances of natural water cycle processes and natural climates. The AR5 of IPCC (2013) pointed out that in the twenty-first century global warming will further intensify the Earth's water cycle, making the high-latitude areas even wetter and mid- and low-latitude areas even drier, melting more glaciers and reducing spring snow covers in the Northern Hemisphere.

In the arid and semiarid areas, the hydrological processes of rivers were sufficiently documented to have responded to global warming sensitively over the past several decades (e.g., Hu et al. 2015; Wang et al. 2013; Myktybekovna et al. 2014). For example, many studies

This article is part of a Topical Collection in Environmental Earth Sciences on "Water in Central Asia," guest edited by Daniel Karthe, Iskandar Abdullaev, Bazartseren Boldgiv, Dietrich Borchardt, Sergey Chalov, Jerker Jarsjö, Lanhai Li and Jeff Nittrouer.

✉ Changchun Xu
xcc0110@163.com

[1] Key Laboratory of Oasis Ecology, School of Resource and Environment Sciences, Xinjiang University, Urumqi 830046, China

[2] State Key Laboratory of Desert and Oasis Ecology, Xinjiang Institute of Ecology and Geography, Chinese Academy of Sciences, Urumqi 830011, China

[3] Xinjiang Tarim River Basin Bayingolin Management Bureau, Korla 841000, China

Published online: 30 July 2016

showed that the river flow originated from high mountains in the arid Central Asia has increased during the past 30 years primarily due to enhanced glacial melting (Hu et al. 2015; Wang et al. 2013; Zhang et al. 2010). However, some rivers that are also originated from high mountains have experienced flow decreases or even disruptions because of the intensified agriculture irrigation-related water interception (Xu et al. 2013; Zhang et al. 2012). Even worse, some terminal lakes have shrunk or even dried up completely. The most well-known terminal lakes that experienced human-resulted shrinkage include the Lop Nor (Yuan and Yuan 1998; Fan et al. 2009), the Taitema Lake (Chen et al. 2003) and the Aral Sea (Deng and Long 2011; Wu et al. 2009). It is apparent that the natural hydrological processes and patterns have been dramatically altered by human-resulted changes in climate and in hydrology. It is undesirably anticipated that the natural hydrological processes and patterns in the arid and semiarid areas will be more dramatically altered by these human-resulted changes. It means that the societies in the arid and semiarid areas will face stronger-than-ever challenges in managing water resources, and thus, the need for predicting future water-resource availability is pressing. This paper is a scenario-based academic exercise attempting to predict future water-resource availability in Kaidu River, one of the headwaters of the Tarim River in southern Xinjiang, Northwest China.

The Kaidu River is the primary river feeding the Bosten Lake, the latter being the largest inland freshwater lake in China. The lake level once reached the record high in 2002 (1049.4 m a.s.l), being 4.6 m higher than the record low in 1986 (1044.8 m a.s.l) primarily because of the increase in temperature. Since 2002, however, the lake level has kept dropping to the present level (1045.0 m a.s.l) mainly due to the decrease in water input caused by upstream water interceptions combined with climate change. It is now a well-accepted paradigm that prediction, planning and management of water resources are becoming increasingly crucial for the big river basins in terms of the security of food production and the health of natural ecosystems. This paradigm is also appealing to the Kaidu River basin. Most previous studies have focused on the past change of hydro-climatic processes in the basin (Chen et al. 2013a; Xu et al. 2008; Tao et al. 2007), but very few on the future change of hydro-climatic processes in the basin. In this paper, the SDSM (Statistical DownScaling Model) and the Statistical Analog Resampling Scheme (STARS) were used to project the future climate scenarios and the Soil and Water Assessment Tool (SWAT) was used to simulate the river runoff changes in the Kaidu River under different climate change scenarios for the future 30 years (2011–2040).

Study area

The Kaidu River is situated on the northeastern edge of the Taklimakan Desert, the second largest desert in the world (Fig. 1). It lies between 41°47′–43°21′N and 82°52′–86°55′E, with a drainage area 4.79×10^4 km^2 and a main river length of 560 km. The river originates from the southern slope of the Tianshan Mountains in Northwest China. It discharges into the Bosten Lake, and the Boston Lake is in turn the headwater of the downstream river, the Konqi River that flows into the Lob Nor. Since the Kaidu River inputting the Boston Lake and the Konqi River outputting the Bosten Lake are hydrologically linked, the linked system (Kaidu–Bosten–Konqi) is thus called the Kaidu–Konqi River basin.

The Kaidu River is the predominant contributor of the Bosten Lake, occupying more than 80 % of the inflowing water. The average annual runoff at the Dashankou hydrological station (a control station at the mountain exit) was 35.05×10^8 m^3 for the period 1961–2010. It supplies water not only for the oasis development of the Kaidu–Konqi river basin but also for the ecological maintenance of the lower reaches of Tarim River.

The Kaidu–Konqi River basin belongs to the continental arid climate. The mean annual temperature was −4.2 °C (Bayanbulak station) in mountainous area and 8.9 °C (Hejing, Yanqi and Bohu stations) in plain area for the period 1961–2010. Precipitation falls mainly between June and August with a large heterogeneity both in time and in space. It generally decreases along a NW–SE transect of decreasing elevations. The mean annual precipitation ranges from 300 mm to 500 mm in mountainous area and decreased to only 50–100 mm in plain area (Chen et al. 2013b).

Materials and methods

Data preparation

Data used for running the SWAT model include the followings: (1) digital elevation model (DEM) with a resolution of 90 × 90 m obtained from the International Scientific Data Service Platform, Chinese Academy of Sciences (http://www.cnic.cn/zcfw/sjfw/gjkxsjjx); (2) land use type (1/100,000) and soil type and properties (1/1,000,000) obtained from the Environmental and Ecological Science Data Center in the West of China (http://westdc.westgis.ac.cn); (3) meteorological data including daily sequences of precipitation, temperature (maximum and minimum), wind velocity, relative humidity and solar radiation at the Bayanbulak meteorological station for the

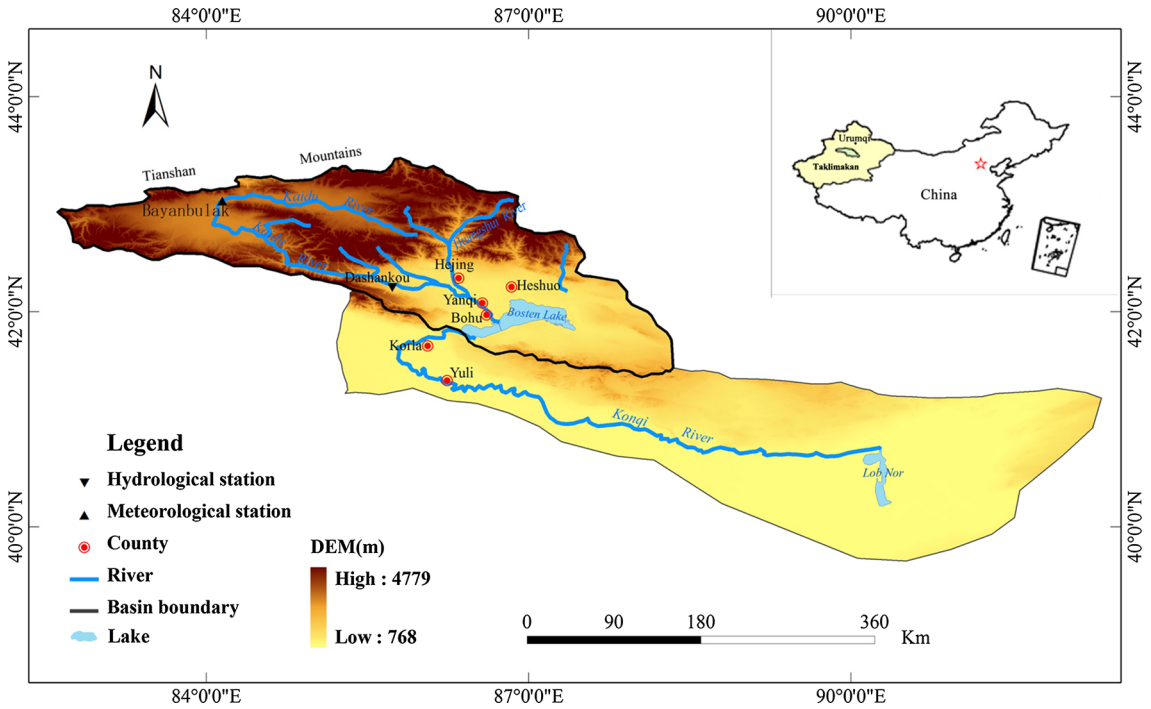

Fig. 1 Sketch map of the study area and hydrological and meteorological stations

period 1961–2010 obtained from China Meteorological Data Sharing Service System (http://data.cma.cn); (4) hydrological data: daily discharge at the Dashankou hydrological station for the period 1981–2010 obtained from Xinjiang Bayingolin Mongol Autonomous Prefecture Water Conservancy Bureau.

Three data sets were used in SDSM. The first was the station meteorological data including daily maximum temperature (T_{max}), daily minimum temperature (T_{min}) and daily precipitation (P) at the Bayanbulak station. The second was National Centers for Environmental Prediction (NCEP) reanalysis data including the grid NCEP reanalysis data sets covering the Bayanbulak station for the period 1961–2000. For the sake of spatial resolution consistency with the data of general circulation model (GCM) outputs, the NCEP data were reinterpolated into a standard coordinate system (2.5° latitude × 3.75° longitude) over the entire watershed. The NCEP data sets contain 26 general circulation factors (i.e., temperature, sea-level pressure, wind speed and direction, 850 and 500 hPa geopotential height field, vorticity, divergence and relative humidity). The third was GCMs data including the HadCM3 developed by the Hadley Center for Climate Prediction and Research in British. The HadCM3 was demonstrated to perform relatively well compared to other models in simulating climate in Asia (Shi et al. 2005). The two emission scenarios of HadCM3, A2 and B2, representing the high and moderate emission levels, were considered to predict runoff variations for the period of 2011–2040.

Models

Soil and Water Assessment Tool

The Soil and Water Assessment Tool (SWAT) is a watershed-scale and processes-based distributed hydrological model developed by the Agricultural Research Service at the US Department of Agriculture. It was developed to quantify the impact of various management strategies on water discharge, sediment and water quality in large complex catchments (Gassman et al. 2007). It can be run in daily, monthly or yearly time steps. In this paper, it was run in daily step to simulate the river flow at the Dashankou station for the period 2011–2040.

The daily flow during 1981–2010 was split into two segments for calibration and validation of the model: 1981–1990 was the calibration period, and 1991–2010 was the validation period. The simulated flows were compared to the observed ones at both daily and monthly scales.

The model performance was evaluated using the Nash–Sutcliffe efficiency (E_{NS}, Nash and Sutcliffe 1970), the percent bias (PBIAS, Moriasi et al. 2007) and the coefficient of determination (R^2).

$$E_{\mathrm{NS}} = 1 - \frac{\sum_1^n \left(Q_i^{\mathrm{obs}} - Q_i^{\mathrm{sim}}\right)^2}{\sum_1^n \left(Q_i^{\mathrm{obs}} - \bar{Q}_i^{\mathrm{obs}}\right)^2} \quad (1)$$

$$\mathrm{PBIAS} = \frac{\sum_1^n \left(Q_i^{\mathrm{obs}} - Q_i^{\mathrm{sim}}\right)}{\sum_1^n Q_i^{\mathrm{obs}}} \times 100\ \% \quad (2)$$

$$R^2 = \left[\frac{\sum_1^n \left(Q_i^{\mathrm{sim}} - \bar{Q}_i^{\mathrm{sim}}\right)\left(Q_i^{\mathrm{obs}} - \bar{Q}_i^{\mathrm{obs}}\right)}{\sqrt{\sum_1^n \left(Q_i^{\mathrm{sim}} - \bar{Q}_i^{\mathrm{sim}}\right)^2}\sqrt{\sum_1^n \left(Q_i^{\mathrm{obs}} - \bar{Q}_i^{\mathrm{obs}}\right)^2}}\right]^2 \quad (3)$$

where Q_i^{obs} and Q_i^{sim} are the ith observed value and simulated value for daily flow, $\bar{Q}_i^{\mathrm{obs}}$ and $\bar{Q}_i^{\mathrm{sim}}$ are the means of observed and simulated data for daily flow, and n is the total number of daily flow observations.

E_{NS} indicates how well the plot of observed versus simulated data fits the 1:1 line. E_{NS} values range between $-\infty$ and 1.0 (1 inclusive), with $E_{\mathrm{NS}} = 1$ being the ideal value. $E_{\mathrm{NS}} > 0.5$ means satisfactory according to Moriasi et al. (2007). PBIAS measures the average tendency of the simulated data to be larger or smaller than their observed counterparts. The optimal value of PBIAS is 0.0, with lower magnitude values indicating more accurate model simulation. Positive values indicate an underestimation of observation, while negative values indicate an overestimation (Gupta et al. 1999). R^2 describes the portion of total variance in the measured data that can be explained by the model. R^2 ranges from 0 to 1, with higher values indicating less error variance, and typically values greater than 0.5 are considered acceptable (Moriasi et al. 2007). In summary, the modeling performance can be categorized or ranked into four levels (Table 1).

Statistical DownScaling Model

The Statistical DownScaling Model (SDSM) is a downscaling tool developed by Wilby et al. (2002) and has been widely used in many fields like meteorology, hydrology and environmental assessment (Abdo et al. 2009; Duan and Mei 2014; Huang et al. 2011; Zuo et al. 2011). In this paper, the SDSM (version 5.2) was used to develop the future climate scenarios of the basin.

Three procedures involved in the SDSM modeling. The first procedure was identification of the screen variable. That is, the seasonal correlation analysis, partial correlation analysis and scatter diagram were used to identify the relationships between the predictor variables (i.e., NCEP variables) and predictands (i.e., precipitation, $T_{\max}$ and $T_{\min}$). The variables that were significantly correlated with predictands were selected as predictors. The second procedure was model calibration. That is, multiple linear regressive equations were established between the predictands and the identified predictors. Since the distribution of daily precipitation is highly skewed, a fourth root transformation was applied to the original precipitation to establish the needed transfer functions. The third procedure was application of transfer functions, i.e., the established transfer functions were used to downscale the outputs from the HadCM3 and validated the regression equations.

Statistical Analog Resampling Scheme

The Statistical Analog Resampling Scheme (STARS) is a resampling approach based on the weather analogs (Orlowsky et al. 2008). It is based on the assumption that weather states from segments of the observation period may occur again or very similar to the occurred weather states during the simulation period. Hence, the simulated series are constructed by resampling from segments of observation series consisting of daily observations. Because the simulated series consist of the observations and fields from the observation period, the physical consistency of both simulated fields and combinations of different variables is ensured. As the only external constraint to the simulated series at a given location, two parameters of a regression line (e.g., mean and slope) are prescribed. They are the parameters that the simulated annual means of a characteristic climate variable at this location have to be featured.

The scheme provides a fast and easy-to-use tool, which, unlike many of its alternatives, is relatively independent on complex driving information (e.g., extensive GCM outputs). As the simulation series consist of station observations, plausible data with respect to every aspect of local weather conditions are generated—a feature which any kind of dynamically generated grid box series lacks. The scheme has been widely adopted in many recent studies (Julia and Friedrich 2015; Orlowskya and Fraedrich 2009; Orlowsky et al. 2010). According to the temperature change range in this century under the different RCP scenarios in AR5 (IPCC 2013) and with the consideration of

Table 1 Criteria for evaluating the performance of SWAT model

Level	E_{NS}	PBIAS (%)	R^2
Very good	$0.75 < E_{\mathrm{NS}} \leq 1.0$	$-10\ \% < \mathrm{PBIAS} < 10\ \%$	
Good	$0.65 < E_{\mathrm{NS}} \leq 0.75$	$-15\ \% < \mathrm{PBIAS} \leq -10\ \%$ or $10\ \% \leq \mathrm{PBIAS} < 15\ \%$	
Satisfactory	$0.50 < E_{\mathrm{NS}} \leq 0.65$	$-25\ \% < \mathrm{PBIAS} \leq -15\ \%$ or $15\ \% \leq \mathrm{PBIAS} < 25\ \%$	>0.5
Unsatisfactory	$E_{\mathrm{NS}} \leq 0.50$	$\mathrm{PBIAS} \leq -25\ \%$ or $\mathrm{PBIAS} \geq 25\ \%$	

climate change of the basin in mountainous area during 1961–2010 (Zhang et al. 2014), the temperature change scenarios in this paper were prescribed as 0, 0.5 and 1 °C for the future 50 years (2011–2060), representing the low (S1), moderate (S2) and high (S3) warming levels, respectively. The climate outputs for the next 30 years (i.e., 2011–2040) were used and analyzed for the hydrological predictions.

Uncertainty analysis method

The cumulative probability was used to quantify the possible impact of climate change on hydrology (Liu and Tao 2012). First, we calculated the relative change percentage of annual runoff to the baseline period (1961–2010) under the five climate scenarios (A2, B2, S1, S2 and S3). Second, we used the cumulative distribution functions (CDFs) to calculate the probability distribution of runoff change.

Results and analysis

Calibration and validation of models

SWAT

By using the Sufi-2 algorithm integrated in the SWAT-CUP, the sensitivity analysis and calibration were carried out. In this study, 28 parameters related to runoff were analyzed and 16 of them were finally chosen to perform the calibration. After automatic and manual calibrations, the optimal values of parameters were obtained. Figures 2 and 3 show the observed and simulated daily flows in calibration and validation periods (1981–1982 was taken as preheat period so that the results were not shown), respectively. The modeling results were assessed by E_{NS}, PBIAS and R^2 indices. Figures 2 and 3 show that the model performed well on both daily and monthly scales in both calibration and validation periods (Table 2). All the indices were within the good or satisfactory levels (Moriasi et al. 2007, also see Table 1). In general, the model performance in simulation was acceptable and can be used for the hydrological simulation.

SDSM

The selected predictor variables for each predictand are shown in Table 3. Both station-observed data and NECP-generated data during 1961–1990 were used to calibrate the model. The coefficient of determination (R^2) and the standard error (SE) offered by the SDSM were used to evaluate the model performance. R^2 reveals the degree of independent variables (predictors) jointly explaining the dependent variable (predictand) in the regression equations. SE mirrors the sensitivity of predictands to predictors.

The R^2 of daily T_{max} and T_{min} regression equations in the calibration period was 0.59 and 0.43, and the SE of them was 3.40 and 3.58 °C, respectively, indicating that the selected predictors can explain the predictands relatively well (Table 4). Compared to the temperatures, the precipitation was explained by the model not very well with R^2 and SE being 0.12 and 0.29 mm, respectively. Similarly, the data of 1991–2000 were used to validate the model. The R^2 of daily T_{max}, T_{min} and P in the validation period was 0.61, 0.49 and 0.15, and the SE of them was 3.35, 3.48 °C and 0.29 mm, respectively.

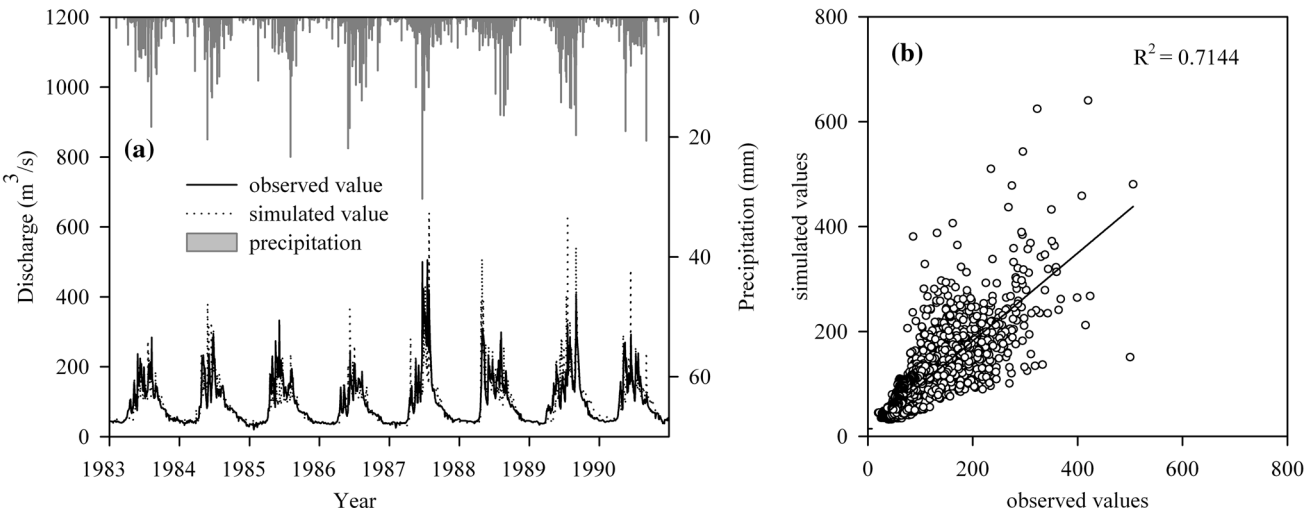

Fig. 2 Observed and simulated daily river flows by the SWAT during the calibration period, 1983–1990. **a** Hydrograph, **b** scatter plots

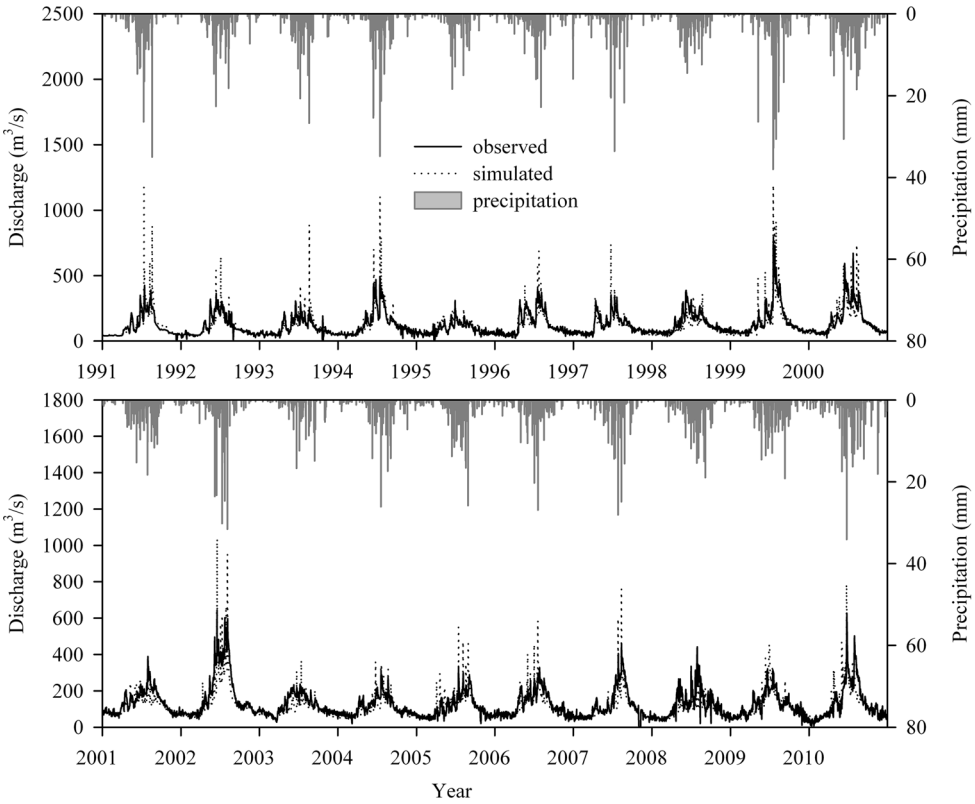

Fig. 3 Observed and simulated daily flows by the SWAT during the validation period, 1991–2010. *Upper panel* precipitation, *lower panel* river discharge

Table 2 Assessment of simulation results by the SWAT model in both calibration and validation periods

Statistics	Scale	E_{NS}	PBIAS (%)	R^2
Calibration (1983–1990)	Daily	0.69	1.05	0.71
	Monthly	0.88	1.98	0.88
Validation (1991–2010)	Daily	0.62	7.41	0.67
	Monthly	0.81	7.74	0.84

Except the statistics (R^2 and SE) offered by the SDSM itself, correlation coefficient (r) was also calculated to evaluate the comparison between the simulated and the observed sequences (Fig. 4). It could be found that the correlation coefficients for temperature simulations were all above 0.96, reaching "very good" level, and the correlation coefficients for monthly precipitation were above 0.38, reaching the relatively satisfactory level (Table 4). Overall, the SDSM performed extremely well in temperature simulation and performed reasonably well in precipitation simulation.

STARS

The daily temperature and precipitation during 1961–2010 at the Bayanbulak station were used to check the performance of STARS in climate projection. The former period (1961–1985) was the training period, and the latter period (1986–2010) was the reference period. Figure 5 shows that the simulated data agreed with the observed ones very well in the reference period. The correlation

Table 3 The optimal predictors screened by the SDSM for the three predictands

Predictand	T_{max}	T_{min}	P	Explanatory note
Predictor	*p_z*	*p_z*	*p_u*	*p_z*: vorticity at surface; *p500*: 500 hPa geopotential height; *p8_z*: vorticity at 850 hPa; *shum*: near surface specific humidity; *temp*: mean temperature at 2 meters high; *p5_u*: zonal velocity at 500 hPa; *r500*: relative humidity at 500 hPa; *r850*: relative humidity at 850 hPa; *p_u:* zonal velocity at surface; *p_zh*: divergence at surface; *p5_z*: vorticity at 500 hPa
	p500	*p5_u*	*p_z*	
	p8_z	*r500*	*p_zh*	
	shum	*r850*	*p5_z*	
	temp	*shum*	*p500*	
			r850	

Table 4 Statistics of simulation results by the SDSM in calibration (1961–1990) and validation (1991–2000) periods

Period	T_{max}			T_{min}			P		
	R^2	SE	r	R^2	SE	r	R^2	SE	r
Calibration	0.59	3.40	0.97	0.43	3.58	0.96	0.12	0.29	0.39
Validation	0.61	3.35	0.96	0.49	3.48	0.96	0.15	0.29	0.38

The temperature series used daily data, and the precipitation series used monthly data

R^2, the coefficient of determination; SE, standard error (°C, mm); r, correlation coefficient between observed and simulated series

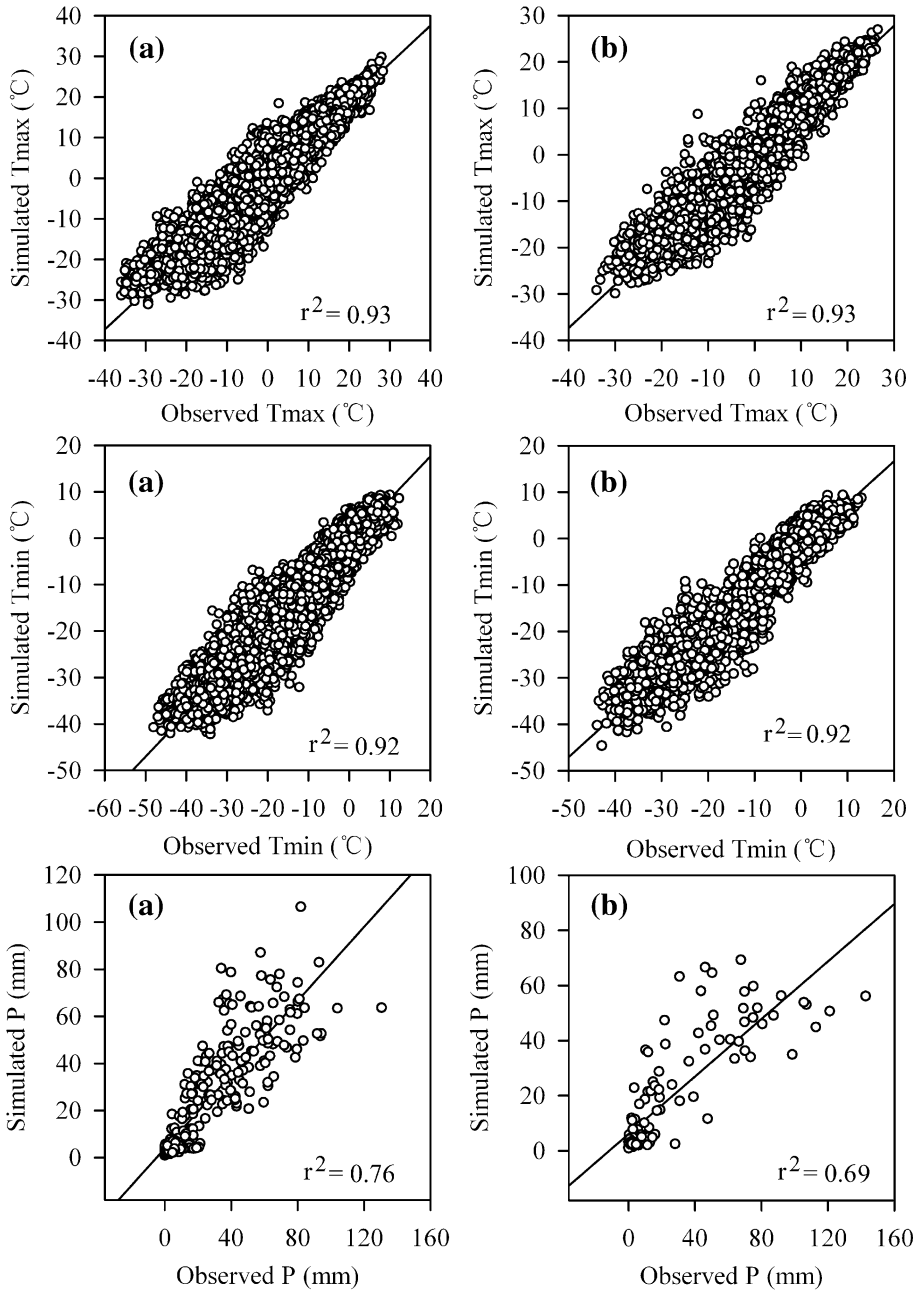

Fig. 4 Comparisons between the simulated and observed values (T_{max}, T_{min}, P) by the SDSM in calibration period (**a**) and validation period (**b**). Temperatures used daily data, and precipitation used monthly data in figures

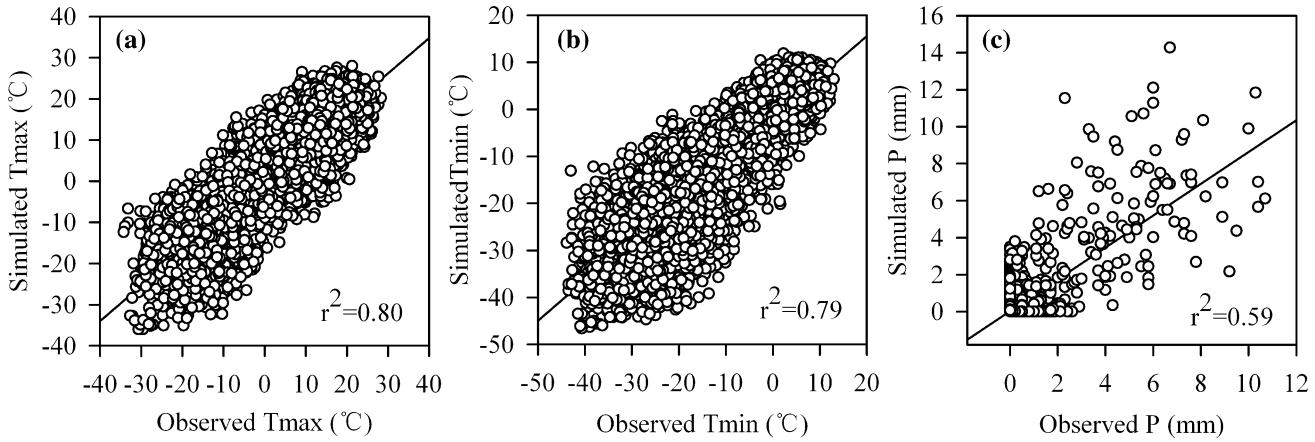

Fig. 5 Comparisons between the observed and simulated values by the STARS model in the reference period (1986–2010). **a** T_{max}, **b** T_{min}, **c** P. Temperatures used daily data, and precipitation used monthly data in figures

coefficients were 0.89, 0.89 and 0.13 for daily T_{max}, T_{min} and P and 0.97, 0.98 and 0.77 for monthly T_{max}, T_{min} and P, respectively. Again, the simulations were better in temperature than in precipitation. In general, the model performed well and can be used in the projection of future climate change.

Projections of future climate scenarios

Annual variations

Based on the validated SDSM and STARS, two sets of future climate scenarios were obtained for the basin. One is obtained by inputting the daily T_{max}, T_{min} and P from the HadCM3 during 2011–2040 into the SDSM to get the station (Bayanbulak) climate scenarios under A2 and B2 emission scenarios (Fig. 6a1–a3). Another is obtained by inputting the three prescribed warming scenarios (S1, S2 and S3) into the STARS to get the corresponding T_{max}, T_{min} and P of the period from 2011 to 2040 at the Bayanbulak station (Fig. 6b1–b3).

The annual variations of the projected T_{max}, T_{min} and P showed large differences between the two sets of climate scenarios. Under A2 and B2 scenarios, both T_{max} and T_{min} appeared strong increasing trends, especially after 2020. However, precipitation did not show any obvious trend. Under the three prescribed warming scenarios, both T_{max} and T_{min} exhibited decreasing trends under S1 and S2 and an increasing trend under S3. The simulated precipitation then showed decreasing trends under S1 and S3 and an increasing trend under S2. Overall, the mean annual T_{max} and T_{min} in the future 30 years differed less between the two sets of climate scenarios than the annual precipitation that has a 70-mm difference between two sets of climate scenarios.

Seasonal variations

The intra-annual variations of the projected variables suggested that there were no large differences in T_{max} and T_{min} among the scenarios and also among the different projecting periods (Fig. 7). The projected temperatures had similar distributions, and the T_{max} and T_{min} ranged within −20 to 20 °C and −30 to 10 °C, respectively. For the projected precipitation, the peaks occurred between June and August for all the scenarios and also all the projecting periods, but the projected amount varied significantly. Under S1–S3, the peak volume could reach 60–80 mm. Under A2 and B2, the volume could only reach ∼50 mm. As for the decadal variability, the precipitation during 2030s is generally lower than that of 2010s and 2020s, suggesting that the future air could become much drier under warming climate.

Runoff prediction

Annual runoff

The runoff (m^3/s) at the Bayanbulak station for the period 2011–2040 was predicted by inputting the five scenario-based projections of daily T_{max}, T_{min} and P. Figure 8 shows the annual runoff (estimated by daily river flows, 10^8 m^3) for both the baseline period 1961–2010 with observed values and the projection period 2011–2040 with simulated values.

The simulated annual runoffs under A2 and B2 fluctuated with relatively small amplitudes (28–49 × 10^8 m^3) compared with those under S1–S3 (22–54 × 10^8 m^3) (Fig. 8). On average, the mean annual runoffs under A2, B2 and S2 during the projection period were larger than the mean annual runoff of the baseline period

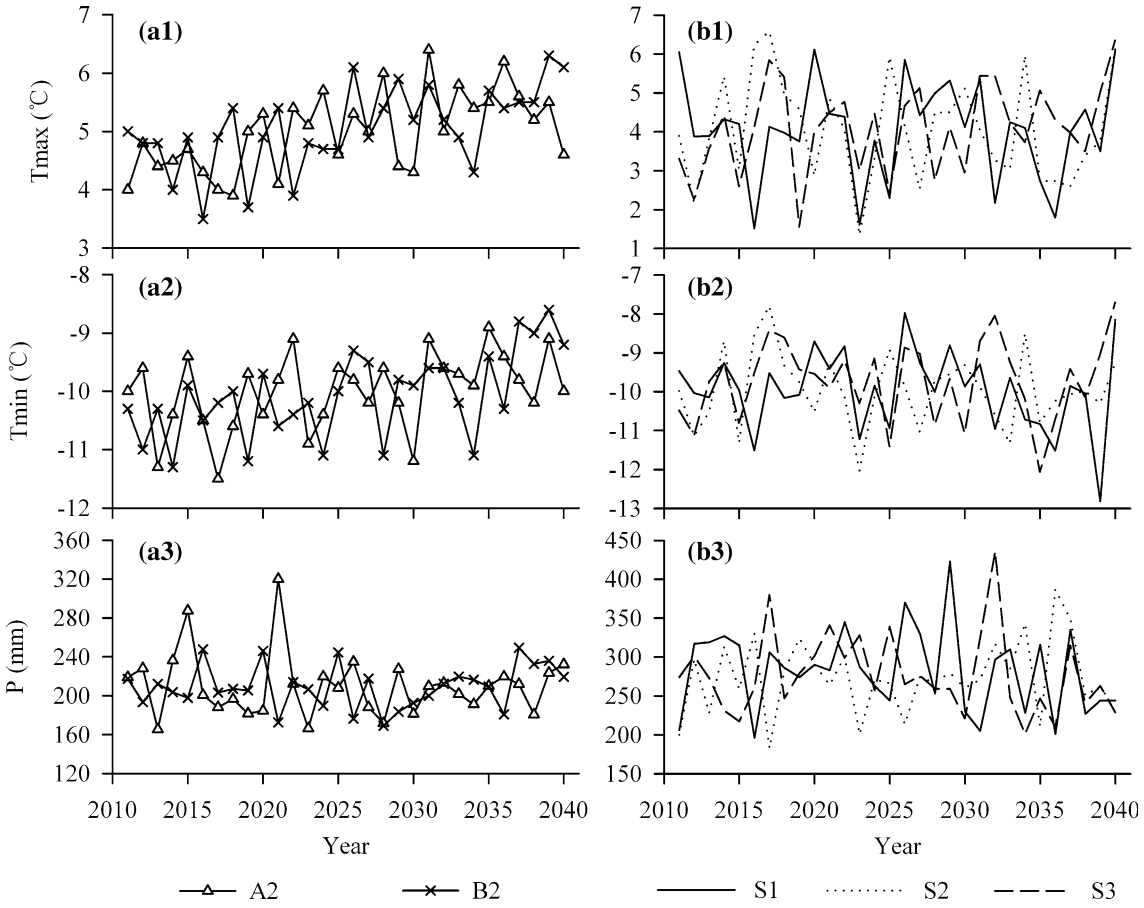

Fig. 6 Annual changes in the projected T_{max} (**a1**, **b1**), T_{min} (**a2**, **b2**) and P (**a3**, **b3**) under A2 and B2 emission scenarios of HadCM3 (*left*) and under the three prescribed climate scenarios (S1, S2 and S3) (*right*) for the period 2011–2040 at the Bayanbulak station. The annual values are shown in figures

(35.05×10^8 m^3) and the mean annual runoffs under S1 and S3 were smaller than that in the baseline period (Table 5), but the difference was not large. It means that the runoff in the future 30 years could be comparable with that in the past ~50 years.

In terms of the decadal change, the projected annual runoffs could reach or exceed the level of baseline period in the coming two decades (2010s and 2020s) under the most scenarios, but in 2030s projected runoff could fall below the level of baseline period. In other words, high emission (A2) or higher (S3) and lower (S1) increasing temperature could be disadvantageous to runoff production in the basin.

Seasonal runoff

The projected seasonal runoff fluctuated dramatically under each of scenarios (Fig. 9). Compared to the projected seasonal runoff fluctuations under the three climate scenarios (S1–S3), the runoff fluctuations under the two emission scenarios (A2 and B2) exhibited stronger trends with smaller amplitudes. Under the high emission level (A2), runoffs in all seasons except spring showed a decreasing trend and were relatively abundant in the coming 20 years (2010s–2020s) and relatively short in the 2030s in comparison with the baseline period. Under the moderate emission level (B2), however, runoffs did not show any significant decreasing or increasing trends. Under the S1–S3 scenarios, runoffs changed dramatically without any significant trends. In contrast, the higher the temperature, the more dramatic the fluctuation was. Taken together, the most scenarios suggested that it is very likely that runoff could decrease during the 2030s, especially in spring and summer when agriculture was badly in need of water.

Uncertainty analysis

The results of cumulative probability distribution function showed that the cumulative probability of runoff increase was 66, 69, 43, 63 and 49 % for A2, B2, S1, S2 and S3 climate scenarios, respectively (Fig. 10). It means that runoff under the two emission scenarios was most likely to

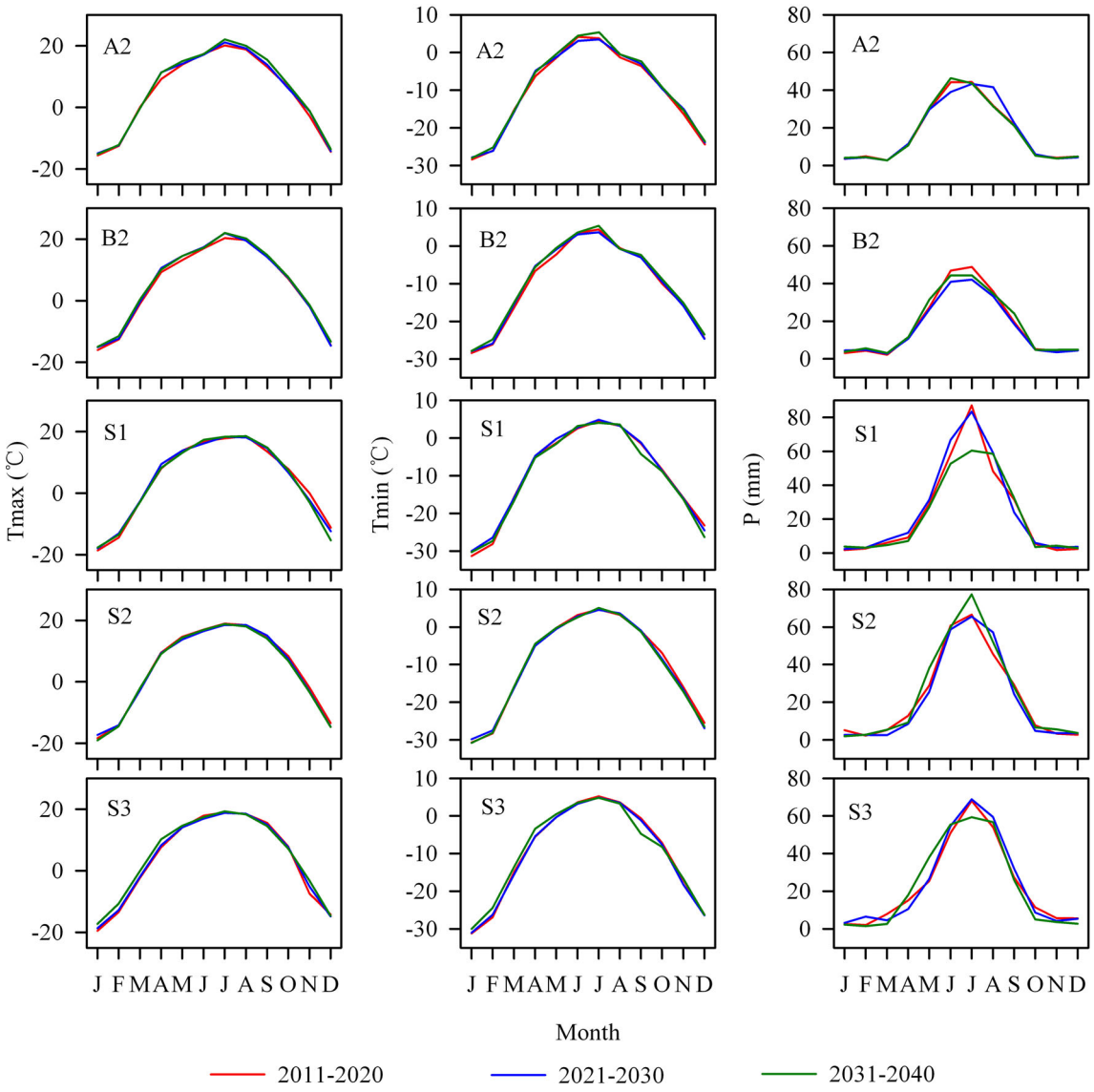

Fig. 7 Intra-annual changes in the projected T_{max} (*left*), T_{min} (*middle*) and P (*right*) under A2, B2, S1, S2 and S3 scenarios for the period 2011–2040 at the Bayanbulak station. *Red line* 2011–2020, *blue line* 2021–2030 and *green line* 2031–2040

increase. But, the cumulative probabilities of runoff increase under S1–S3 indicated that the moderate warming (S2) but neither the lower (S1) nor the higher (S3) warming was conducive to the runoff increase.

Discussion

Water-resource prediction is essential for the future sustainable development of an area. It is especially the case for arid and semiarid areas where water resource is a constraining factor for the sustainable development. In this paper, the runoff change of the Kaidu River, an inland river in Northwest China, was predicted for the future 30 years (2011–2040) by the SWAT hydrological model and the SDSM and STARS downscaling models. The modeling results suggest that the SWAT model can perform well in runoff simulation in the basin, further proving the suitability of SWAT model applied in the arid region as previous studies (Zhao et al. 2015; Lu et al. 2012; Huang and Zhang 2010; Chen et al. 2009). However, it still should be noted that the SWAT model itself is not capable of simulating the glacier's melting process. In this paper, glaciers were treated as snow in simulation, which may have some impacts on results though glaciers are not much in our study area. A suitable ice module should be studied and embedded into the SWAT model in our future work for more accurate results.

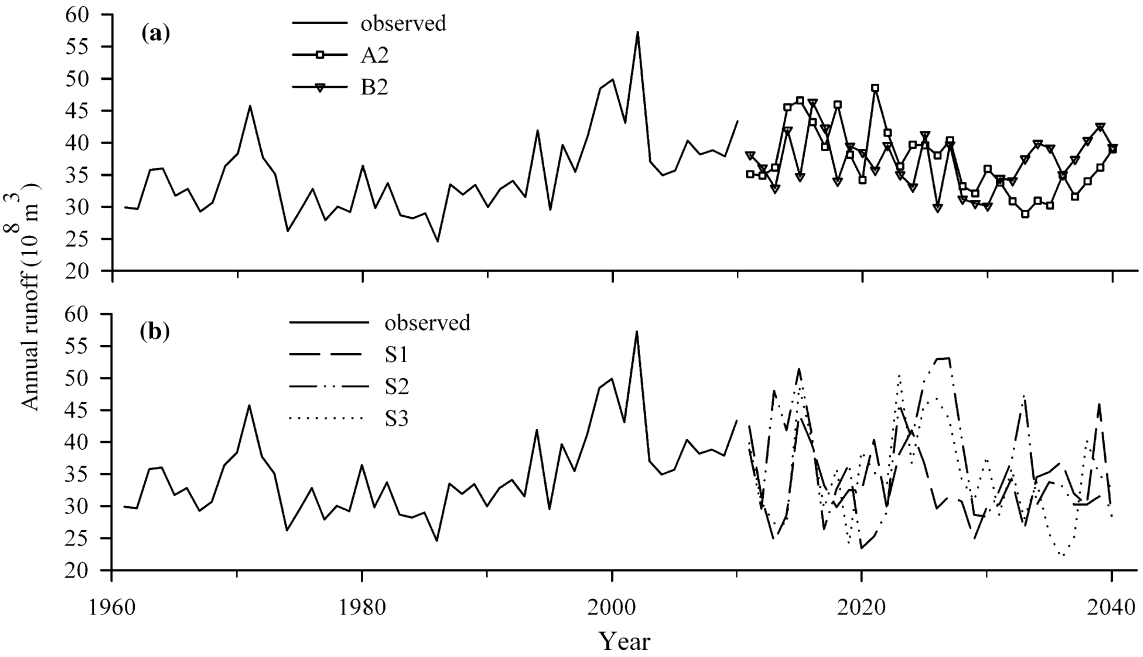

Fig. 8 The simulated annual runoff under A2 and B2 emission scenarios (**a**) and S1–S3 prescribed climate scenarios (**b**) during the forecast period 2011–2040, together with the observed values during the baseline period 1961–2010

Table 5 The simulated mean annual runoff (10^8 m^3) at the Bayanbulak station of Kaidu River during the forecast period 2011–2040 under the five climate scenarios

	A2	B2	S1	S2	S3
2011–2020	39.92	38.45	33.90	37.00	34.20
2021–2030	38.54	34.63	33.33	39.40	39.47
2031–2040	33.04	37.99	33.40	33.57	30.67
Average	37.17	37.02	33.55	36.66	34.78

A2: high emission level; B2: moderate emission level; S1: $\Delta T = 0$ °C; S2: $\Delta T = 0.5$ °C; S3: $\Delta T = 1$ °C

Downscaling techniques are critical to the accuracy of future climate projection and then runoff prediction. Clearly, both SDSM and STARS have been shown performing extremely well in temperature simulation and reasonably well in precipitation simulation in this paper. The common problem in many current studies is that the simulation and prediction precision of hydrological variables especially precipitation is rather low, which then causing poor simulation of runoff. The lower precision of precipitation simulation is often associated with the particularity and irregularity of precipitation processes. How to reduce the uncertainty of precipitation is still one of the difficulties in current climate change and water cycle research (Xia et al. 2011).

The projections of future climate scenarios show that the basin will experience a significant increase in air temperature and an indistinctive change in precipitation under A2 and B2 scenarios, which probably means that the study area will experience a drying trend in the future 30 years. Meanwhile, the relatively abundant predicted runoff from 2010s to 2020s but obviously short after 2020s under A2 scenario also seems to verify the drying trend. The drying is predicted to be shown especially in spring and summer when agricultural is badly in need of water, which will affect the sustainable development of social economy of the basin. Thus, water shortage should be prevented in advance, e.g., building more reservoirs in mountains for not only storing water but also reducing the evaporation losses. Compared with the high emission level (A2), runoffs under the moderate emission level (B2) did not show any significant increasing or decreasing trends. The moderate emission level is more beneficial to the maintenance of runoff.

Under the prescribed S1–S3 scenarios, temperature (T_{max} and T_{min}), precipitation and runoff did not conformably increase accompanied with the increasing prescribed mean temperature from S1 to S3. The precipitation and runoff under the moderate warming scenario (S2) had a relatively large increase compared with that under low warming scenario (S1) and high warming scenario (S3). High warming is not in favor of the precipitation and runoff generations. More importantly, high warming often increases runoff rapidly by the fast glacier melting in the short term, but in the long run the melt water will drop sharply as glaciers melt especially in the area with more

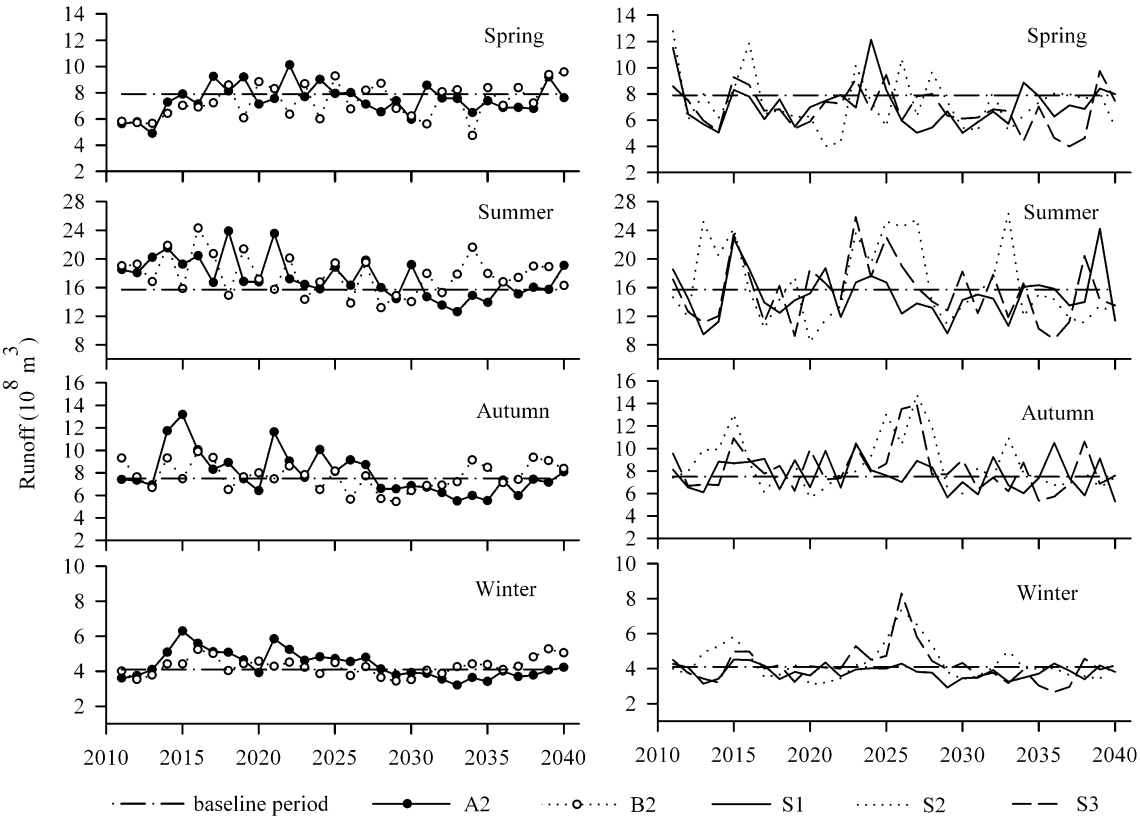

Fig. 9 The simulated seasonal runoff under A2 and B2 emission scenarios (**a**) and S1–S3 prescribed climate scenarios (**b**) during the forecast period 2011–2040

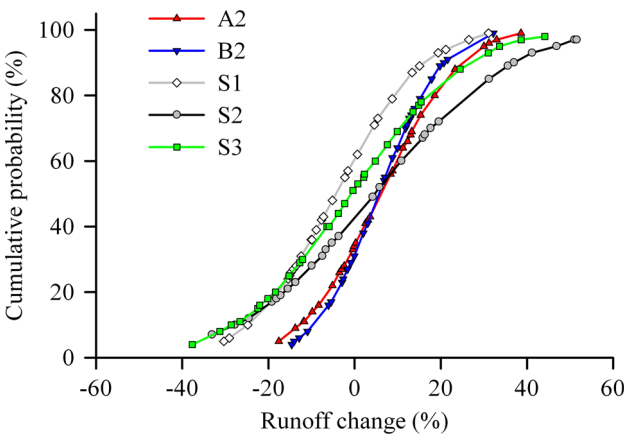

Fig. 10 The cumulative probabilities of runoff change under the five scenarios

small glaciers which are easy to disappear. In the Kaidu River basin, there are 832 glaciers, but most of them have an area of 0.1–0.5 km^2. Oppositely, low warming is also not conductive to the precipitation and runoff generations because of the slow water cycle. Thus, the moderate warming (S2) but neither the lower (S1) nor the higher (S3) warming was beneficial to the runoff increase.

Uncertainty research is a difficulty in global climate change and water resources impact assessment (Coquard et al. 2004; Taylor 2005). Uncertainties can originate from many aspects, including GCMs, downscaling methods, hydrological models and parameters and the greenhouse gas emission scenarios (Wilby and Harris 2006; Kay et al. 2009; Chen et al. 2011). In this study, all of these uncertainties are involved but not assessed, which may affect the accuracy and reliability of results. The uncertainty analysis should be strengthened in our future work. Additionally, the biggest uncertainty often comes from GCMs followed by downscaling method (Wilby and Harris 2006), so an integrated model with multiple GCMs together with different downscaling techniques should be tried to reduce the errors caused by any one model or technique.

Conclusions

Based on the hydro-meteorological data over the past 50 years (1961–2010), the runoff change of the Kaidu River was predicted for the future 30 years (2011–2040) by the SWAT hydrological model and the SDSM and STARS

two downscaling techniques. The primary conclusions were drawn as follows.

1. The SWAT model can well duplicate the recorded runoff changes in the basin, with the E_{NS}, PBIAS and R^2 all reaching the satisfactory level. It can be applied to the simulation of future runoff changes.
2. Both the SDSM and the STARS models performed well in simulating temperature but relatively poorly in simulating precipitation. Under the A2 and B2 scenarios the basin will experience a significant increasing trend in temperature and an indistinctive change trend in precipitation during the projection period (2011–2040). Under the S1–S3 scenarios, both temperature and precipitation do not exhibit distinctive changes during the period of 2011–2040.
3. The predicted average annual runoff will be relatively abundant during the period from 2010s to 2020s but obviously short after 2020s under A2 scenario. The decreasing trends from 2010s to 2030s are shown in each season. The runoff will be kept steady under B2 scenario. Under S1–S3 scenarios, the runoff will fluctuate drastically without any significant trend. The runoff is relatively high under S2 scenario.
4. Both the scenario-based predictions and the cumulative probability distribution function suggest that moderate emission (e.g., B2) or moderate warming (e.g., S2) is beneficial to maintaining the expected level of runoff in the future.

Acknowledgments This study is jointly supported by the National Natural Science Foundation (Nos. 41561023, 41305125, 41271052) and the Open Fund of State Key Laboratory of Desert and Oasis Ecology, Xinjiang Institute of Ecology and Geography, Chinese Academy of Sciences (G2013-02-02). Thanks to the data sharing of the International Scientific Data Service Platform, Chinese Academy of Sciences (http://www.cnic.Cn/zcfw/sjfw/gjkxsjjx), the Environmental and Ecological Science Data Center in the West of China (http://westdc.westgis.ac.cn) and the China Meteorological Data Sharing Service System (http://data.cma.cn). Special thanks are owed to the editors and anonymous reviewers for their detailed and constructive comments.

References

Abdo KS, Fiseha BM, Rientjes THM, Gieske ASM, Haile AT (2009) Assessment of climate change impacts on the hydrology of Gilgel Abay catchment in Lake Tana basin, Ethiopia. Hydrol Process 23:3661–3669

Chen YN, Cui WC, Li WH, Zhang YM (2003) Utilization of water resources and ecological protection in the Tarim River. Acta Geogr Sin 58(2):215–222 **(in Chinese)**

Chen L, Xu ZX, Luo R, Mi YJ (2009) SWAT application in arid and semi-arid region: a case study in the Kuye River basin. Geogr Res 28(1):65–73 **(in Chinese)**

Chen J, Brissette FP, Leconte R (2011) Uncertainty of downscaling method in quantifying the impact of climate change on hydrology. J Hydrol 401:190–202

Chen YN, Du Q, Chen YB (2013a) Sustainable water use in the Bosten Lake basin. Science Press, Beijing

Chen ZS, Chen YN, Li BF (2013b) Quantifying the effects of climate variability and human activities on runoff for Kaidu River Basin in arid region of northwest China. Theor Appl Climatol 111(3–4):537–545

Coquard J, Dun PB, Taylor KE (2004) Simulations of western U.S. surface climate in 15 global climate models. Clim Dyn 23:455–472

Deng MJ, Long AH (2011) Water resources issue among the Central Asia countries around the Aral Sea: conflict and cooperation. J Glaciol Geocryol 33(6):1376–1390 **(in Chinese)**

Duan K, Mei Y (2014) A comparison study of three statistical downscaling methods and their model-averaging ensemble for precipitation downscaling in China. Theor Appl Climatol 116:707–719

Fan ZL, Alishir K, Xu HL, Zhang QQ, Abdumijiti (2009) Changes of Tarim River and evolution of Lop Nur. Quat Sci 29(2):232–242 **(in Chinese)**

Gassman PW, Reyes MR, Green CH, Arnold JG (2007) The soil and water assessment tool: historical development, applications, and future research directions. Trans ASABE 50(4):1211–1250

Gupta HV, Sorooshian S, Yapo PO (1999) Status of automatic calibration for hydrologic models: comparison with multilevel expert calibration. J Hydrol Eng 4(2):135–143

Hu ZD, Wang L, Wang ZJ, HongY Zheng H (2015) Quantitative assessment of climate and human impacts on surface water resources in a typical semi-arid watershed in the middle reaches of the Yellow River from 1985 to 2006. Int J Climatol 35:97–113

Huang QH, Zhang WC (2010) Application and parameters sensitivity analysis of SWAT model. Arid Land Geogr 33(1):8–15 **(in Chinese)**

Huang J, Zhang JC, Zhang ZX, Xu CY, Wang BL, Yao J (2011) Estimation of future precipitation change in the Yangtze River basin by using statistical downscaling method. Stoch Environ Res Risk Assess 25:781–792

IPCC (2013) Working Group I Contribution to the Fifth Assessment Report of the Intergovernmental Panel on Climate Change. In: Stocker TF, Qin DH, Plattner GK, Tignor M, Allen SK, Boschung J, Nauels A, Xia Y, Bex V, Midgley PM (eds) Climate change 2013: the physical science basis. Cambridge University Press, Cambridge

Julia L, Friedrich WG (2015) Improving seasonal matching in the STARS model by adaptation of the resampling technique. Theor Appl Climatol 120(3–4):751–760

Kay AL, Davies HN, Bell VA, Jones RG (2009) Comparison of uncertainty sources for climate change impacts: flood frequency in England. Clim Change 92:41–63

Liu YJ, Tao FL (2012) Probabilistic Assessment and uncertainties analysis of climate change impacts on wheat biomass. Acta Geogr Sin 67(3):337–345 **(in Chinese)**

Lu ZX, Cai XH, Zou SB, Long AH, Xu BR (2012) Application of SWAT model in the upstream of Ili River Basin with scarce data. Arid Land Geogr 35(3):399–407 **(in Chinese)**

Moriasi DN, Arnold JG, Van Liew MW, Bingner RL, Harmel RD, Veith TL (2007) Model evaluation guidelines for systematic quantification of accuracy in watershed simulations. Trans ASABE 50(3):885–900

Myktybekovna SN, Chen YN, Salamat A (2014) Climate change and its impact on the hydrological processes of the Talas River in central Asia. Fresen Environ Bull 23(6):1423–1432

Nash JE, Sutcliffe JV (1970) River flow forecasting through conceptual models: part I. a discussion of principles. J Hydrol 10:282–290

Orlowsky B, Gerstengarbe FW, Werner PC (2008) A resampling scheme for regional climate simulations and its performance compared to a dynamical RCM. Theor Appl Climatol 92(3–4):209–223

Orlowsky B, Bothe O, Fraedrich K, Gerstengarbe FW, Zhu XH (2010) Future climates from bias-bootstrapped weather analogs: an application to the Yangtze River basin. J Clim 23(13):3509–3524

Orlowskya B, Fraedrich K (2009) Upscaling European surface temperatures to North Atlantic circulation-pattern statistics. Int J Climatol 29(6):839–849

Shi XY, Xu XD, Xu Y (2005) Comparison of temperature between six hundreds stations in China and output of IPCC models. Meteorology 31(7):49–53

Tao H, Wang GY, Shao C, Song YD, Zou SP (2007) Climate change and its effects on runoff at the headwater of Kaidu River. J Glaciol Geocryol 29(3):413–417 **(in Chinese)**

Taylor K (2005) IPCC Coupled Model Output for Working Group 1. In: Workshop on analysis of climate model simulations for IPCC AR4, Honolulu, Hawaii

Wang HJ, Chen YN, Li WH, Deng HJ (2013) Runoff responses to climate change in arid region of northwestern China during 1960–2010. Chin Geogr Sci 23(3):286–300

Wilby RL, Harris I (2006) A framework for assessing uncertainties in climate change impacts: low-flow scenarios for the River Thames, UK. Water Resour Res 42:W02419. doi:10.1029/2005WR004065

Wilby RL, Dawson CW, Barrow EM (2002) SDSM—a decision support tool for the assessment of regional climate change impacts. Environ Model Soft 17:147–159

Wu JL, Ma L, Jilili A (2009) Lake surface change of the Aral Sea and its environmental effects in the arid region of the Central Asia. Arid Land Geogr 32(3):418–422 **(in Chinese)**

Xia J, Liu CZ, Ren GY (2011) Opportunity and challenge of the climate change impact on the water resource of China. Adv Earth Sci 26(1):1–12 **(in Chinese)**

Xu JH, Chen YN, Ji MH, Lu F (2008) Climate change and its effects on runoff of Kaidu River, Xinjiang, China: a multiple timescale analysis. Chin Geogr Sci 18(4):331–339

Xu CC, Chen YN, Chen YP, Zhao RF, Ding H (2013) Responses of surface runoff to climate change and human activities in the arid region of Central Asia: a case study in the Tarim River basin, China. Environ Manag 51(4):926–938

Yuan GY, Yuan L (1998) An approach to the environmental changes in Lop-Nur history. Acta Geogr Sin 53(sup.):83–89 **(in Chinese)**

Zhang Q, Xu CY, Tao H, Chen David YQ (2010) Climate changes and their impacts on water resources in the arid regions: a case study of the Tarim River basin, China. Stoch Environ Res Risk Assess 24(3):349–358

Zhang XH, Yang DG, Xiang XY, Huang X (2012) Impact of agricultural development on variation in surface runoff in arid regions: a case of the Aksu River basin. J Arid Land 4(4):399–410 **(in Chinese)**

Zhang YN, Xu CC, Li WH, Zhao J (2014) Climate change characteristics and impacts on surface runoff in the Kaidu River Basin. Sci Soil Water Conserv 12(1):81–89 **(in Chinese)**

Zhao J, Xu CC, Gao ST, Li JX (2015) Hydrological modeling in the Urumqi River basin based on SWAT. Arid Land Geogr 38(4):666–674 **(in Chinese)**

Zuo DP, Xu ZX, Li JY, Liu ZF (2011) Spatiotemporal characteristics of potential evapotranspiration in the Weihe River basin under future climate change. Adv Water Sci 22:455–461 **(in Chinese)**